Parameter space of experimental chaotic circuits with high-precision control parameters

Francisco F. G. de Sousa, Rero M. Rubinger, José C. Sartorelli', Holokx A. Albuquerque, and Murilo S. Baptista

Citation: Chaos **26**, 083107 (2016); doi: 10.1063/1.4960582
View online: http://dx.doi.org/10.1063/1.4960582
View Table of Contents: http://aip.scitation.org/toc/cha/26/8
Published by the American Institute of Physics

Parameter space of experimental chaotic circuits with high-precision control parameters

Francisco F. G. de Sousa,[1] Rero M. Rubinger,[1] José C. Sartorelli,[2,a)]
Holokx A. Albuquerque,[3] and Murilo S. Baptista[4]
[1]*Instituto de Física e Química, Universidade Federal de Itajubá, Itajubá, MG, Brazil*
[2]*Universidade de São Paulo, São Paulo, SP, Brazil*
[3]*Departamento de Física, Universidade do Estado de Santa Catarina, Joinville, SC, Brazil*
[4]*Institute of Complex Systems and Mathematical Biology, SUPA, University of Aberdeen, Aberdeen, United Kingdom*

(Received 23 March 2016; accepted 25 July 2016; published online 8 August 2016)

We report high-resolution measurements that experimentally confirm a spiral cascade structure and a scaling relationship of shrimps in the Chua's circuit. Circuits constructed using this component allow for a comprehensive characterization of the circuit behaviors through high resolution parameter spaces. To illustrate the power of our technological development for the creation and the study of chaotic circuits, we constructed a Chua circuit and study its high resolution parameter space. The reliability and stability of the designed component allowed us to obtain data for long periods of time (∼21 weeks), a data set from which an accurate estimation of Lyapunov exponents for the circuit characterization was possible. Moreover, this data, rigorously characterized by the Lyapunov exponents, allows us to reassure experimentally that the shrimps, stable islands embedded in a domain of chaos in the parameter spaces, can be observed in the laboratory. Finally, we confirm that their sizes decay exponentially with the period of the attractor, a result expected to be found in maps of the quadratic family. *Published by AIP Publishing.*
[http://dx.doi.org/10.1063/1.4960582]

Electronic circuits provide a simple alternative to test in the laboratory theoretical approaches developed to characterize more complex systems. So far, however, experiments were being carried out in circuits with course-grained parameter values. In this work, we present a novel electronic architecture for a potentiometer that permits fine variations in control parameters. To demonstrate the usefulness of this potentiometer to the behavioral analysis of electronic circuits, we make very long time-series measurements of this circuit for a fine variation of its parameters and experimentally report, for the first time, that stable islands embedded in a domain of chaos in the parameter spaces indeed have sizes that decay exponentially with the period of the attractor. Periodicity with high period, confirmed by the calculation of the Lyapunov exponents, thus requires fine tuning of parameters to be experimentally observed.

I. INTRODUCTION

Only a few chaotic circuits have periodicity high resolution parameter spaces experimentally obtained.[1–7] The relevance of studying parameter spaces of nonlinear systems is that it allows us to understand how periodic behavior, chaos, and bifurcations come about in a nonlinear system. In fact, parameters leading to the different behaviors are strongly correlated. Chaotic and periodic regions appear side by side in all scales in universal shapes and forms. Gallas[8] numerically observed periodic structures embedded in parameter chaotic regions, in the parameter space of the Hénon map. For some classes of nonlinear systems, such as the one studied here, the periodic structures appear aligned along spiral curves describing parameters for saddle-node bifurcations and super-stable behavior and that cross transversely parameter curves containing homoclinic bifurcations.[9–14]

Experimentally, the difficulty in obtaining parameter spaces resides in a reliable method to vary precisely a parameter, usually a resistance, in a controlled, autonomous, and reproducible fashion. Parameters are not constant and suffer time varying alterations. This factor becomes even more severe when the experiment is done over long time spans. Finally, the numerical resolution of the parameters and their nominal values cannot be achieved or reproduced experimentally. Even very simple nonlinear electronic systems cannot have their behaviors reproduced numerically; the main reason is that the electronic components have non-ideal characteristic curves. These factors are behind our motivation to propose an approach to obtain experimental parameter spaces that are not only reliable, autonomous, and reproducible but that can also reproduce nominal parameter values considered in numerical experiments. High resolution parameter space[7] allows one to reproduce experimentally the self-similar topological character observed in numerically obtained parameter spaces.

Previous works have proposed different strategies to construct experimental parameter spaces. Maranhão *et al.* considered a manual or step motor control of precision multi-turn potentiometer.[1] Stoop *et al.*[5,6] used a proto-board

a)Electronic mail: sartorelli@if.usp.br

to do the experiment and varied by hand 490×162 values of a negative resistor and an inductor to produce parameter spaces. In Ref. 2, a Keithley power source controlled by LabView® was used as one parameter and a precision potentiometer manually controlled as the second parameter. The use of a digital potentiometer would provide a reliable, autonomous, and reproducible way to obtain parameter spaces. However, the available digital potentiometers on the market are limited to resistances above 1 kΩ and usually not more than 256 steps are possible. In addition, their control is not easy to carry out with typical data acquisition (DAQ) systems or LabView®. The novelty in our experimentally obtained parameter spaces is that they are constructed by calculating the spectrum of Lyapunov exponents from reconstructed attractors, considering long-time series of measured trajectories.

The technological novelty presented is the design of a digital potentiometer with precisely calibrated small resistance steps (as low as 0.10022 Ω) that allows 1024 steps (or even more) to change the resistance. With these potentiometers and a set of resistors, switches, and relays, we were able to autonomously obtain a high resolution parameter space of the Chua's circuit (with resolutions of 400×562 and 1023×126 points, varying one resistor with step sizes of 0.200001 Ω and another with 0.10022 Ω), which could remarkably reproduce the numerically obtained parameter spaces. This new electronic component allowed us to carry out a detailed experimental investigation of the parameter space of a modified Chua's circuit, namely, we have characterized this circuit by varying the resistance (R) and the inductor resistance (r_L).[15,16] Among other accomplishments, we have demonstrated that even higher period periodic windows and the complex topological structure of the scenario for the appearance of periodic behaviors can be observed experimentally. Simulations, considering a normalized equation set that models the Chua's circuit and also the normalized version of the experimental i(V) curve, were carried out in order to demonstrate that the occurrence of periodic structures observed in the high-resolution experimental parameter space could also be numerically observed. In particular, we showed by calculating the Lyapunov exponents numerically and experimentally that this parameter space presents self-similar periodic structures, the shrimps, embedded in a domain of chaos.[1–8,10,11,13,14] We also show experimentally that those self-similar periodic regions organize themselves in period-adding bifurcation cascades, and whose sizes decrease exponentially as their period grows.[1,9,17,18] We also report on malformed shrimps on the experimental parameter space, result of tiny nonlinear deviations close to the junction of two linear parts from a symmetric piecewise linear i(V) curve.

We have considered Chua's circuit,[19] with 5 linear parts, to perform our study experimentally and numerically because this circuit has been studied in many applications such as in chaos control,[20,21] synchronization[22,23] and others, but the use of a higher precision potentiometers here proposed can be used to characterize, study, and precisely control the behavior of any electronic equipment.

II. EXPERIMENTAL AND NUMERICAL ASPECTS

Let us start describing the digital potentiometer. Its diagram is presented in Fig. 1, but only 3 of the set of 10 resistors in series are shown to illustrate its structure. The 10 pin left connector stands for the digital data coming from input/output (I/O) digital ports of the DAQ board. A 60 Ah 12.0 V car battery was used to drive the digital potentiometers. The digital potentiometer idea was captured from the structure of

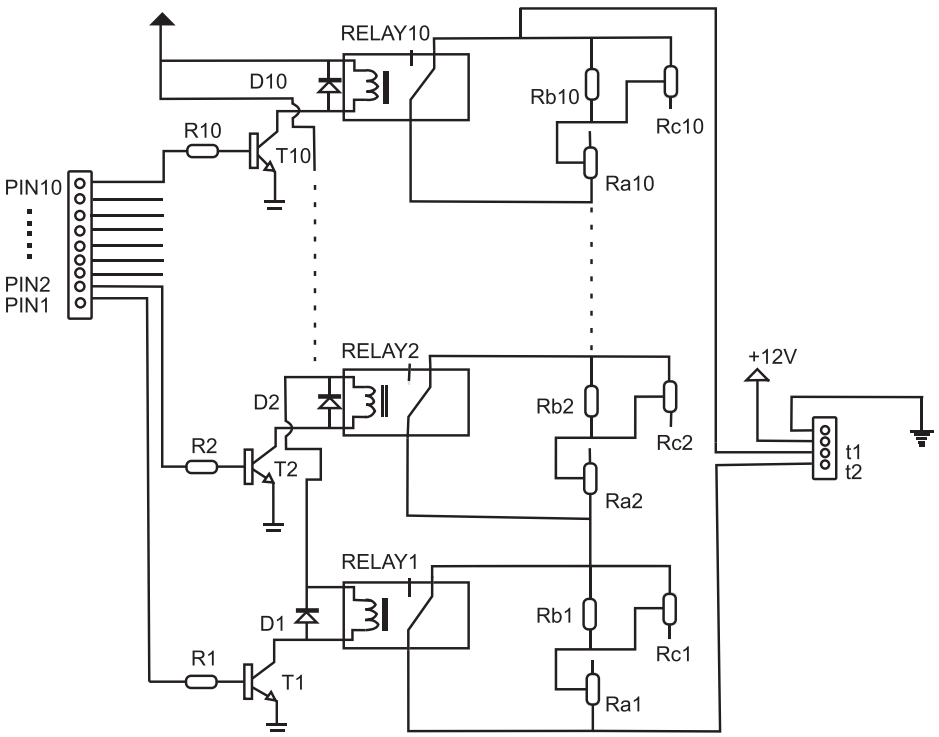

FIG. 1. Schematics of the designed adjustable digital potentiometer. Only three of ten resistor circuits of the in series association are shown in order to clearly present their components. On the right connector, t1 and t2 represent the output resistance to be connected to the Chua's circuit. The circuit is feed by 60 Ah 12.0 V car battery. See text for component and respective function description.

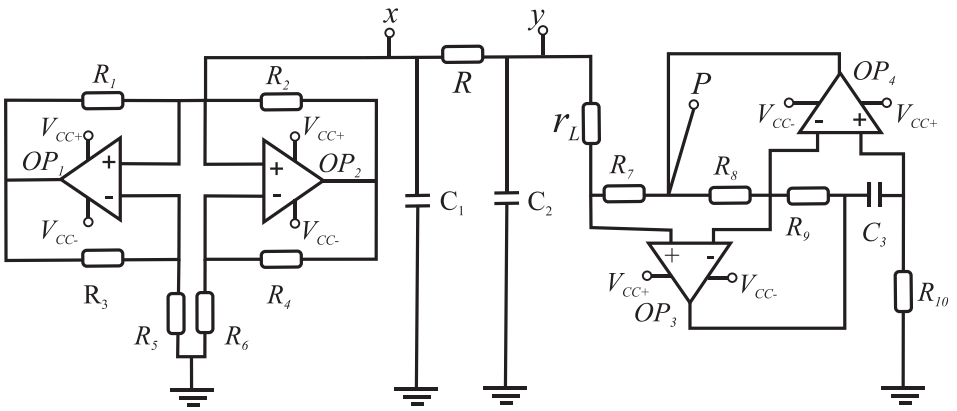

FIG. 2. Chua's circuit using the electronic inductor and indicating the measuring points x, y and the P point. The current through the inductor is defined as $I_L = (V_P - V_{C2})/(R_7 + r_L)$. Here, $V_{cc+} = +12\,\text{V}$ and $V_{cc-} = -12\,\text{V}$.

a switched resistor digital to analog converter which contains a parallel resistor network. The calibration was done using a Keithley digital multimeter model 2001 in the four wire mode, i.e., in order to subtract leads resistance. The relays of the series association were switched by transistor driver circuits connected to I/O digital ports of the data acquisition board used for control and data acquisition. Thus, it was possible to write a ten digit binary number in order to select one of the 1024 possible combinations. The digital potentiometer is used to provide the resistances R and r_L in the circuit, which take up values $R = r$ and $r_L = r$ by following the equation:

$$r = step * (bit0 * 2^0 + bit1 * 2^1 + \cdots + bit9 * 2^9). \quad (1)$$

For R we used two-step values: $0.20001\,\Omega$ and $2.00002\,\Omega$ and for r_L just one value for step, i.e., $0.10022\,\Omega$.

The Chua's circuit scheme is presented in Fig. 2, constructed in a single face circuit board with the same scheme of Ref. 24, i.e., $C_1 = 23.50\,\text{nF}$, $C_2 = 235.0\,\text{nF}$, and $L = 42.30\,\text{mH}$. These values were obtained from the combination of passive commercial available components and measured with a Keithley digital multimeter model 2001 or an impedance analyzer for the reactive components. The measurement of components allowed the choice of the closest possible values to components, better than the factory precision. We evaluate the oscillation main frequency as a rough approximation by $1/(2\pi(LC_2)^{1/2})$ which gives 1596 Hz. Further increase on frequency, i.e., by reducing passive component values, seems to destroy periodic structures that are observed in this circuit, thus this oscillation frequency was the best choice. It was built with TL084 Operational Amplifiers (OPAMPs) and was fed by two 12.0 V, 7 Ah no-break batteries.

The five-fold piecewise linear element that provides the nonlinear character of the Chua's circuit consists of two operational amplifiers (OPAMP) and the resistances R_1 to R_6. Its $i(V_{C1})$ characteristic curve was defined and normalized by the scheme $x = V_{C1}/B_P$ and $i_d(x) = i(x)/(m_0 B_P)$ with $m_0 = -4.156315\,\text{mS}$ and $B_P = 1.38501\,\text{V}$. Here, S stands for the inverse resistance unity. This curve is presented in Fig. 3, with 5-fold linear fittings used for simulations with the significant digits limited by the fitting accuracy, given by

$$i_d(x) = \begin{cases} -32.51240 - 4.76600x & x < -5.43000, \\ x - 0.82999 & -5.43000 \le x < -1.00000, \\ 1.84957x & |x| \le 1.00000, \\ x + 0.86378 & 1.00000 < x \le 5.92900, \\ 37.35590 - 5.15200x & x > 5.92900. \end{cases} \quad (2)$$

The electronic inductor is defined by two OPAMPs connected to the resistors R_7, R_8, R_9, R_{10}, and r_L together with the capacitor C_3. This is a gyrator circuit with inductance as $L = (C_3 R_7 R_9 R_{10})/R_8$.

The points in the circuit where we take measurements can be seen in Fig. 2 by the probe points x, y, and P. They correspond to the voltages across the capacitors C_1 and C_2 and the third variable, the current I_L, is obtained from the relation $I_L = (V_P - V_{C2})/(R_7 + r_L)$, where V_P is the voltage indicated by the P probe. The voltage across C_1, passed by a simple OPAMP buffer, was measured by a National

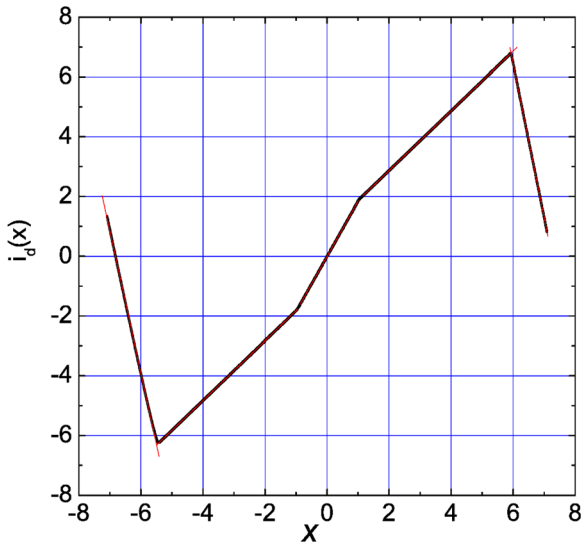

FIG. 3. $i_d(x)$ characteristic of the circuit presented in Fig. 2. The linear fittings are presented in the figure. The equations corresponding to linear fittings are presented in the experimental section. The normalization considered equations $x = V_{C1}/B_P$ and $i_d(x) = i(x)/(m_o B_P)$ and the parameters $m_o = -4.156315\,\text{mS}$ and $B_P = 1.38501\,\text{V}$.

Instruments data acquisition (DAQ) interface, model PCI-6259 with 16 bit resolution, maximum sampling rate of 1.25 Msamples/s, for data storage. Also, LabView was used to data acquisition and analysis.[2,3] A Keithley 2400 voltage/current source in series with the Chua's diode was applied to obtain the i(V) data.

For each time series, the potentiometers R and r_L were switched by a LabView routine with values previously determined and calibrated to give precise equivalent steps. After calibration, the 1024 values of each potentiometer were tested with a linear fitting, giving slopes equal to steps up to four significant digits. We have carried out experiments with the Chua's circuit recollecting time series for the calculation of the Lyapunov exponents. Time series were generated with a 50 Ksamples/s and a 7 s length. As transient, after setting the pair of parameters R and r_L, a 50 s waiting time was considered. It is worth commenting that data acquisition to obtain 562×400 meshes of time series lasted 21 weeks.

The fact that the experimental circuit could reproduce many relevant structures obtained numerically implies that the general bifurcation scenario of these periodic windows of the parameter space is robust to external perturbations and should be expected to be observed in nature. The circuit is not switched off between subsequent measurements, only at the highest R value when recharge was necessary. Each restart of the system has changed the attractor initial conditions. However, because the parameters were varied from high R to lower R values and from low r_L to higher r_L values, the trajectory at restart was always going towards the same fixed points or simple periodic orbits. By starting at parameters leading to such attractors provides results as if the system was never switched off. Thus, this form of covering the parameter space allows best reproducibility since the next attractor for a renewed set of parameters has its initial condition from the state of the circuit set with parameters very close to those parameters. This allows the experiments and the simulations to be performed without any experimental or numerical discontinuity in the state variables.

Experimental characteristic curves of the Chua's circuit are often asymmetric. However, some authors have done simulations by considering a symmetric piecewise-linear function. For us, successful reproduction of the experimental parameter spaces is also a consequence of the fact that our correspondent simulations were performed by considering the non-symmetric $i_d(x)$ give in Eq. (2) to integrate Chua's differential equations. We have considered the same set of differential equations and normalized parameters presented in full detail in Ref. 14.

III. RESULTS AND DISCUSSION

The parameter space in Fig. 4(a) shows by colors the values of the largest Lyapunov exponent λ, calculated by the method of Sano and Sawada[25] from the 400×562 experimental time series with R and r_L as the control parameters. The simulated parameter space in Fig. 4(b) considered also the values of λ obtained from time series generated by 1600 values of R and 562 values of r_L in the same range of the experimental data. In the case of simulations, λ was obtained

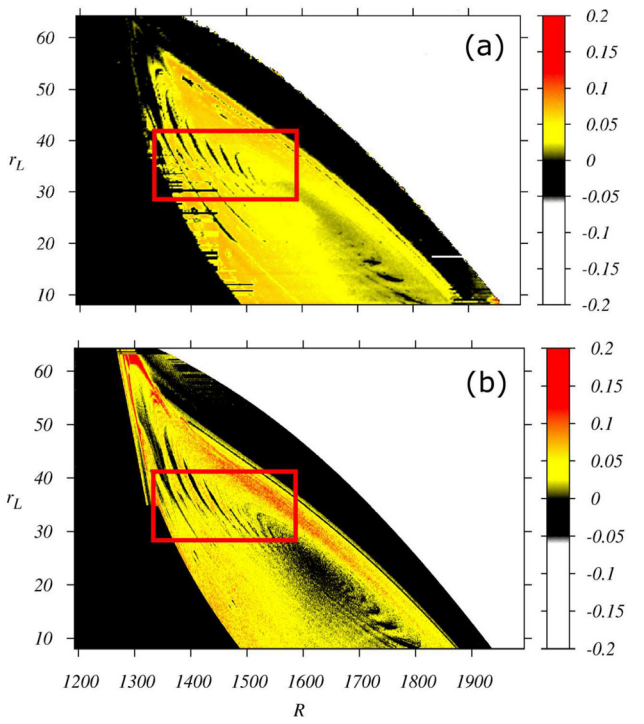

FIG. 4. Lyapunov parameter spaces of the Chua's circuit. White to black stands for periodic orbits and for fixed points; yellow to red color for chaotic orbits. (a) Experimental parameter space diagram associating color scale to λ. Resolution of parameters R and r_L is 2 Ω and 0.1 Ω, respectively, and we have considered a mesh with 400 values for R and 562 values for r_L. (b) Corresponding simulated parameter space obtained from using the model of Ref. 15 but with a 5-fold piece-wise $i_d(x)$ Eq. (2). Resolution of parameters R and r_L is 0.5 Ω and 0.1 Ω, respectively, and we have considered a mesh with 1600 values for R and 562 values for r_L.

from the tangent space method, and the values are in units of integration step. This form of calculating λ allows faster simulations but produces absolute values of the exponents distinct from the corresponding experimental values. The time unit of the experimental Lyapunov exponent was rescaled to match the exponents from numerical data. A larger range parameter space is presented in Fig. 4(a). In Fig. 4(b), we present the correspondent simulations, generated with a 0.10022 Ω step, as described in Section II. The color scales were defined for the experimental data with a smooth color variation from white to black to represent the range of values of λ, with $\lambda < 0$, corresponding to fixed point and periodic attractors, and from black to red to represent the range of values $\lambda \in [0, 0.2]$. The transition between periodic to chaotic orbits occurring through saddle-node bifurcations or through a period doubling cascade is characterized by the shift of colors between yellow and orange. In both parameter spaces of Fig. 4, it is possible to identify the occurrence of complex periodic structures embedded in a chaotic domain and organized in a spiral structure.[8,13,26]

We can see, in Fig. 5, high-resolution amplifications of the inner region of the red boxes shown in Fig. 4. Figure 5(a) shows the experimental data, obtained with a 0.20001 Ω resolution in R. This parameter space has ten times the R resolution as compared with that used in Fig. 4(a). In Fig. 5(b), we present a parameter space constructed by considering a 600×600 mesh of values for R and r_L for the corresponding

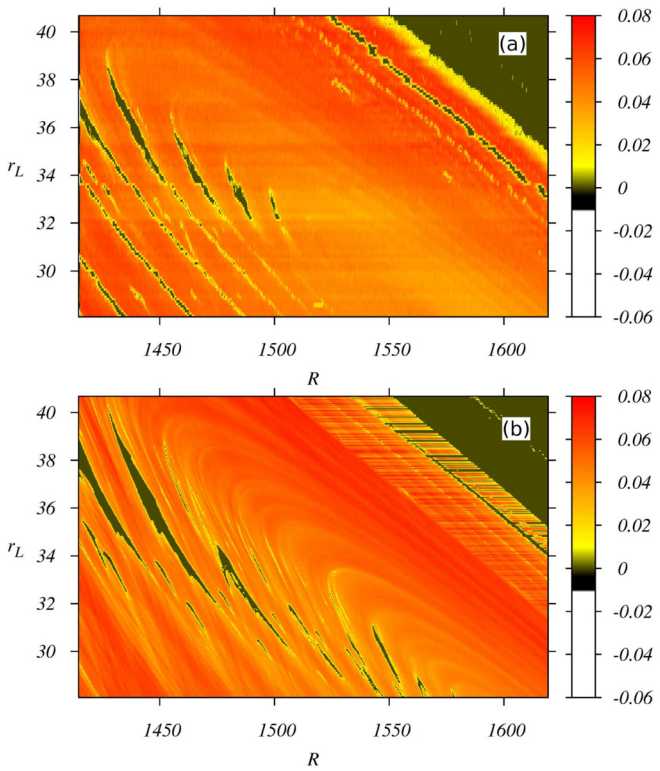

FIG. 5. Magnification of Figs. 4(a) and 4(b). Color scheme is the same used in Fig. 4. In (a). experimental data with ten times the R resolution compared with that used in Fig. 4(a). In (b), a 600×600 mesh parameter space with the same high resolution of the parameter R.

simulations. Notice that both figures are remarkably similar, showing the same complex features. In particular, both figures show details of the complex self-similar organization of periodic regions. Simulations in fact cannot capture all features of the experiments. These features of experimental nature are a noise in the color distribution of the parameter space that makes the boundaries to chaos of the complex periodic windows distorted. This is associated with thermal, electrical noise and the unavoidable analog to digital conversion noise. We estimated from the measured time series that this noise is between 1 mV and 2 mV. This represents three to six times the least significant bits of the DAQ board which is close to the minimum noise experimentally realizable. The second effect is associated with temperature and initial conditions. Between consecutive days, the temperature may vary a few °C and this changes the values of resistances and the diode and the voltage of transistors inside the OPAMPs. We have experienced that the changes are minimum in the component values for a 10 °C change, a variation rarely observed during the measurements. Digital potentiometers were calibrated by adjusting each in series resistor to the closest multiple of 2^n of the step as possible. The accuracy of the step was determined by linear fittings of the resistance versus step plot. The precision on potentiometer steps at constant temperature are about 10 ppm with errors of 20 ppm and 7 ppm specifically. The 1 Ω step potentiometer is fitted as $(1.00001 \pm 0.00002)\Omega$; the 0.2 Ω step potentiometer as $(0.20001 \pm 0.00002)\Omega$; and the 0.1 Ω step potentiometer as $(0.10022 \pm 0.00001)\Omega$. The external ambient temperature changes 11 °C between the minimal and maximal temperature of a day most of the year in the city of Itajubá. In a closed environment as our laboratory, this change is, however, smaller and about 6 °C. Considering this information, we used 10 °C as a maximal temperature variation and obtained from datasheet of resistors and capacitors used that this represents a 250 ppm per °C change in resistors, a 600 ppm per °C change in capacitors, and a drift of 0.018 mV per °C change in the typical 3 mV input offset voltage of the TL084 OPAMP used. This represents a change of 0.00250 Ω on the 1.00001 Ω step digital potentiometer. Our ability to reproduce specific parameters of an experiment is so accurate that we can identify tiny shade variations of the Lyapunov exponent associated to temperature variations.

We have also studied the topological properties of the periodic windows appearing in the parameter spaces of Fig. 4. For that, we created the periodicity parameter spaces in Fig. 6(a), for the experimental time-series, and in Fig. 6(b), for numerical time-series, indicating by colors the period P of the such attractors. In Fig. 7, we verify the existence of expected scaling laws for the largest width of the periodic windows ΔR as a function of the period P of the corresponding attractors in the parameter spaces of Fig. 4, by fitting the following scaling:

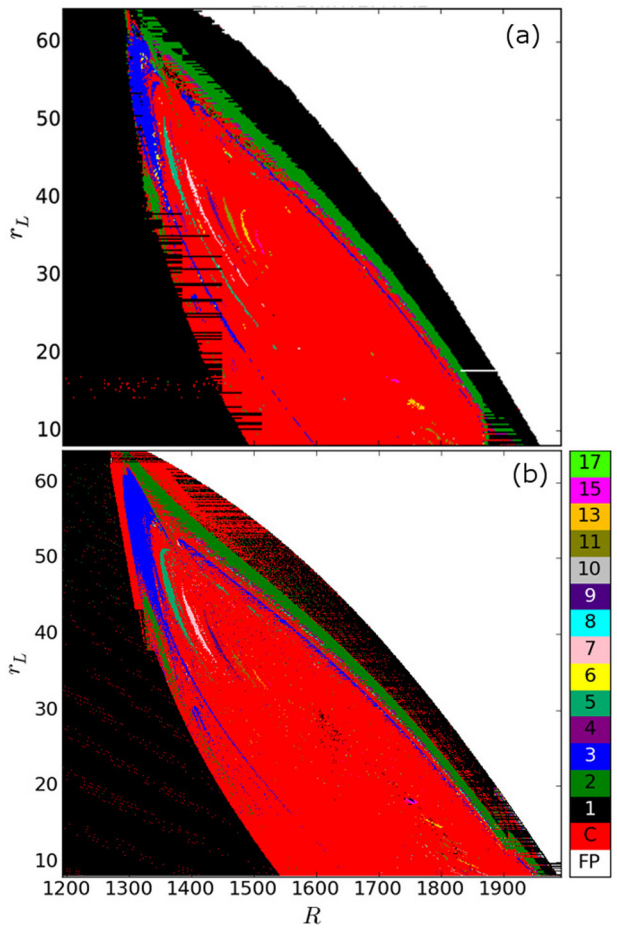

FIG. 6. Periodicity parameter spaces. Color code for the period of the attractor is presented in the right-hand side band. Notice an odd period-adding bifurcation cascade initiating at the top left corner and heading towards the center of the spiral.

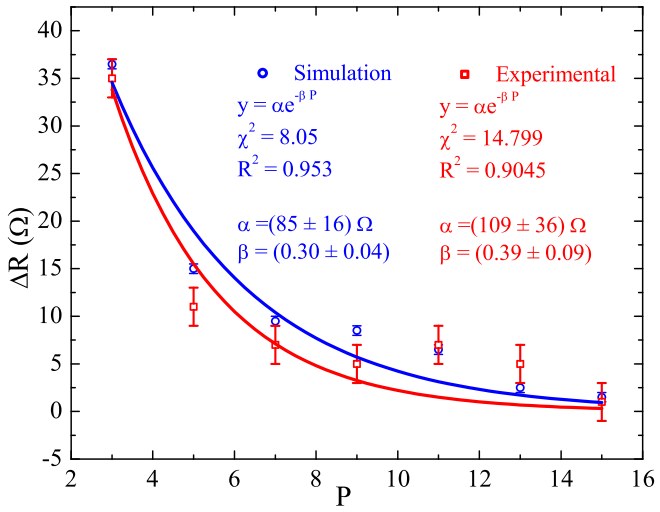

FIG. 7. Fitting of the periodic window largest width ΔR with respect to the attractor period P, considering the exponential scaling of Eq. (3). We considered the error bars of 2 Ω in the experimental calculations and 0.5 Ω in the simulated ones.

$$\Delta R = \alpha e^{-\beta P}, \tag{3}$$

with α and β representing fitting parameters. This result led us to conclude that our experimentally and numerically obtained periodic windows have a complex structure as expected in Refs. 1, 2, 9, and 27. It can be seen from Fig. 6 that periodic windows organize themselves in an odd period adding bifurcation cascade starting from the top left corner of the parameter space towards the spiral center, and whose attractors present period varying from 3 to 17. Window sizes reduce as the period increases and their width ΔR in Ω reaches its minimal value of 2 Ω for periods 15 and 17. Fitting results in Fig. 7 indicate that the decay exponents, $\beta = 0.30 \pm 0.04$ (experimental results) and $\beta = 0.39 \pm 0.09$ (numerical results), are in the same order of magnitude of the largest positive Lyapunov exponent of the chaotic attractor in the chaotic regions surrounding the shrimps, as expected.[1,17] According to Ref. 17, the structure and decay rate of the shrimp sizes is related to their surrounding positive Lyapunov exponents, by $\Delta R = \alpha e^{-2Ph_T H}$, where h_T is the topological entropy of the chaotic attractors (in units of Poincaré crossings) appearing for parameters neighboring the periodic regions and $H = \frac{\tilde{h}_p}{h_T}$, with $\tilde{h}_p$ representing the Lyapunov exponent of the periodic windows measured at the superstable point (in units of Poincaré crossings). We denote $\tilde{\lambda}$ to be the positive Lyapunov exponent of the chaotic attractors appearing for parameters neighboring the periodic regions, but in units of Poincaré crossings, calculated by $\tilde{\lambda} = \lambda \langle T \rangle$, where $\langle T \rangle$ is the average return time of the chaotic trajectory to a Poincaré section. Notice that in Figs. 4 and 5, the Lyapunov exponent is in units of time. For the quadratic map family, $H \approxeq 1$, which we adopt in this work. We also notice that h_T is an upper bound for the largest Lyapunov exponent, so $h_T \geq \tilde{\lambda}$. Therefore, if we estimate β in Eq. (3) by

$$\tilde{\beta} = 2\tilde{\lambda}, \tag{4}$$

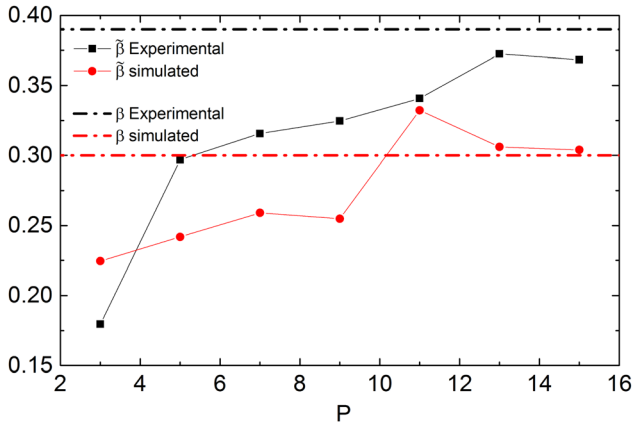

FIG. 8. Estimation of the decay exponent, $\tilde{\beta}$, from the positive Lyapunov exponents of attractors appearing along the border of the shrimps with the chaotic regions as a function of their periods (see Eq. (4)). Black squares stand for experimental values (based on Fig. 4) and red circles for simulations (based on Fig. 5). The dashed black and red lines represent the scaling exponent β, measured from the fittings in Fig. 7, for experimental and simulation data, respectively. For these calculations, we have considered the Lyapunov exponent in units of log(exp) per Poincaré crossing. Notice that in Figs. 4 and 5 the shown Lyapunov exponent is in units of bits per time unit.

we will conclude that $\tilde{\beta} \leq \beta$. In fact, as one can see from Fig. 8, we have that for most of the points $\tilde{\beta} \leq \beta$. This confirms that the scenario we have observed numerically and experimentally in the Chua's circuit follows the same expected scaling laws for periodic windows, believed to be general for quadratic maps.[17]

IV. CONCLUSIONS

We have successfully built autonomous, reliable, and reproducible digital potentiometers that allowed precise measurements of the set of experimental physical parameters of electronic circuits. As an application of the power of our component, we obtained high-resolution experimental parameter spaces of Chua's circuit that is remarkably similar to the one obtained by simulations using the same set of physical parameters values. Two of these specially designed digital potentiometers were used to vary the circuit main resistances and the inductor-resistance, and due to their thermal stability in the experimental parameter spaces we could obtain islands of periodicity embedded in a domain of chaos, the shrimps, whose size windows decay exponentially with the period of the attractors. To the best of our knowledge, this work provides, for the first time, experimental Lyapunov exponent parameter spaces of a spiral cascade structure of several shrimps of electronic circuits. Also, with respect to simulations, we show that considering features such as 5-fold $i_d(x)$ and careful consideration of its equations drawn directly from measurements, it was performed simulations with results close to the ones measured experimentally with regard to the shape of the periodic structures, its exponential decay law, as well as the overall range of Lyapunov exponent values. The very high precision and stability on the resistance steps improved the definition of periodic structure borders when compared with other methods of parameter variation. With the structures in the parameter spaces

well-defined, the exponential decay law of their characteristic sizes against periodicity, expected to be found in quadratic maps, was determined with the results close to those of the simulations.

ACKNOWLEDGMENTS

The authors thank Professor Iberê Luiz Caldas for the suggestions and encouragement. The authors F.F.G.d.S., R.M.R., J.C.S., and H.A.A. acknowledge the Brazilian agency CNPq and state agencies FAPEMIG, FAPESP, and FAPESC, and M.S.B. also acknowledges the EPSRC Grant Ref. No. EP/I032606/1.

[1]D. M. Maranhão, M. S. Baptista, J. C. Sartorelli, and I. L. Caldas, Phys. Rev. E **77**, 037202 (2008).
[2]E. R. Viana, Jr., R. M. Rubinger, H. A. Albuquerque, A. G. de Oliveira, and G. M. Ribeiro, Chaos **20**, 023110 (2010).
[3]E. R. Viana, Jr., R. M. Rubinger, H. A. Albuquerque, F. O. Dias, A. G. de Oliveira, and G. M. Ribeiro, Nonlinear Dyn. **67**, 385–392 (2012).
[4]A. Sack, J. G. Freire, E. Lindberg, T. Pöschel, and J. A. C. Gallas, Sci. Rep. **3**, 3350 (2013).
[5]R. Stoop, P. Benner, and Y. Uwate, Phys. Rev. Lett. **105**, 074102 (2010).
[6]R. Stoop, S. Martignoli, P. Benner, R. L. Stoop, and Y. Uwate, Int. J. Bifurcation Chaos Appl. Sci. Eng. **22**, 1230032 (2012).
[7]A. L'Her, P. Amil, N. Rubido, A. C. Martí, and C. Cabeza, Eur. Phys. J. B **89**, 81 (2016).
[8]J. A. C. Gallas, Phys. Rev. Lett. **70**, 2714–2717 (1993).
[9]R. O. Medrano-T. and I. L. Caldas, e-print arXiv:1012.2241.
[10]G. M. Ramírez-Ávila and J. A. C. Gallas, Phys. Lett. A **375**, 143–148 (2010).
[11]R. Vitolo, P. Glendinning, and J. A. C. Gallas, Phys. Rev. E **84**, 016216 (2011).
[12]R. Barrio, F. Blesa, S. Serrano, and A. Shilnikov, Phys. Rev. E **84**, 035201 (2011).
[13]C. Cabeza, C. A. Briozzo, R. Garcia, J. G. Freire, A. C. Marti, and J. A. C. Gallas, Chaos, Solitons Fractals **52**, 59–65 (2013).
[14]H. A. Albuquerque and P. C. Rech, Int. J. Circuit Theory Appl. **40**, 189–194 (2012).
[15]L. A. Tôrres and L. A. Aguirre, Electron. Lett. **36**, 1915–1916 (2000).
[16]H. A. Albuquerque, R. M. Rubinger, and P. C. Rech, Physica D **233**, 66–72 (2007).
[17]B. R. Hunt and E. Ott, J. Phys. A: Math. Gen. **30**, 7067 (1997).
[18]M. Joglekar, E. Ott, and J. A. Yorke, Phys. Rev. Lett. **113**, 084101 (2014).
[19]L. O. Chua, J. Circuits, Syst. Comput. **4**, 117–159 (1994).
[20]T. Wu and C. Min-Shin, Physica D **164**, 53–58 (2002).
[21]C. D. Campos, R. M. Palhares, E. M. A. M. Mendes, L. A. B. Torres, and L. A. Mozelli, Int. J. Bifurcation Chaos Appl. Sci. Eng. **17**, 3199–3209 (2007).
[22]J. Zhang, C. Li, H. Zhang, and J. Yu, Chaos, Solitons Fractals **21**, 1183–1193 (2004).
[23]Y. Zhang and J. Sun, Phys. Lett. A **330**, 442–447 (2004).
[24]R. M. Rubinger, A. W. M. Nascimento, L. F. Mello, C. P. L. Rubinger, N. Manzanares Filho, and H. A. Albuquerque, Math. Probl. Eng. **2007**, 83893–83909.
[25]M. Sano and Y. Sawada, Phys. Rev. Lett. **55**, 1082–1085 (1985).
[26]J. C. D. Cardoso, H. A. Albuquerque, and R. M. Rubinger, Phys. Lett. A **373**, 2050–2053 (2009).
[27]J. H. Lu, G. R. Chen, and D. Z. Cheng, Int. J. Bifurcation Chaos Appl. Sci. Eng. **14**, 1507–1537 (2004).